

# Molecular spintronics using single-molecule magnets

A revolution in electronics is in view, with the contemporary evolution of the two novel disciplines of spintronics and molecular electronics. A fundamental link between these two fields can be established using molecular magnetic materials and, in particular, single-molecule magnets. Here, we review the first progress in the resulting field, molecular spintronics, which will enable the manipulation of spin and charges in electronic devices containing one or more molecules. We discuss the advantages over more conventional materials, and the potential applications in information storage and processing. We also outline current challenges in the field, and propose convenient schemes to overcome them.

## LAPO BOGANI AND WOLFGANG WERNSDORFER

Institut Néel, CNRS & Université Joseph Fourier, BP 166, 25 Avenue des Martyrs, 38042 GRENOBLE Cedex 9, France

e-mail: wolfgang.wernsdorfer@grenoble.cnrs.fr

The contemporary exploitation of electronic and spin degrees of freedom is a particularly promising field both at fundamental and applied levels<sup>1</sup>. This discipline, called spintronics, has already seen the passage from fundamental physics to technological devices in a record time of ten years, and holds great promise for the future<sup>2</sup>. Spintronic systems exploit the fact that the electron current is composed of spin-up and spin-down carriers, which carry information encoded in their spin state and interact differently with magnetic materials. Information encoded in spins persists when the device is switched off, can be manipulated without using magnetic fields and can be written using low energies, to cite just a few advantages of this approach. New efforts are now directed to obtaining spintronic devices that preserve and exploit quantum coherence, and fundamental investigations are shifting from metals to semiconducting<sup>2,3</sup> and organic materials<sup>4</sup>. The latter is currently used in applications such as organic light-emitting diode (OLED) displays and organic transistors. The concomitant trend towards ever-smaller electronic devices, having already passed the nanoscale, is driving electronics to its ultimate molecular-scale limit<sup>5,6</sup>, which offers the possibility of exploiting quantum effects.

In this context, a new field of molecular spintronics is emerging that combines the ideas and the advantages of spintronics and molecular electronics<sup>7</sup>. The key point is the creation of molecular devices using one or a few magnetic molecules. Compounds of the single-molecule magnet (SMM) class<sup>8,9</sup> seem particularly attractive: their magnetization relaxation time is extremely long at low temperatures, reaching years below 2 K (ref. 8). These systems, combining the advantages of the molecular scale with the properties of bulk magnetic materials, look attractive for high-density information storage and also, due to their long coherence times<sup>10,11</sup>, for quantum computing<sup>12-14</sup>. Moreover, their molecular nature leads to appealing quantum effects of the static and dynamic magnetic properties<sup>15-17</sup>. The rich physics behind the magnetic behaviour produces interesting effects such as negative differential conductance and complete current suppression<sup>18,19</sup>, which could be used in electronics. In addition, specific functions (for

example, switchability with light, electric field and so on) could be directly integrated into the molecule.

This progress article aims to point out the potential of SMMs in molecular spintronics, as recently revealed by experimental and theoretical work, and to delineate future challenges and opportunities. We first show the unique chemical and physical properties of SMMs and then present three basic molecular schemes that demonstrate the state of the art of the emerging field of molecular spintronics. We propose possible solutions to existing problems, and particular emphasis is laid on the motivations and expected results. In the sideboxes, we summarize the quantum properties of SMMs (Box 1) and the basics of molecular electronics (Box 2).

## CHARACTERISTICS OF SINGLE-MOLECULE MAGNETS

SMMs possess the correct chemical characteristics to overcome several problems associated with molecular junctions. They consist of an inner magnetic core with a surrounding shell of organic ligands<sup>8,9</sup> that can be tailored to bind them on surfaces or into junctions<sup>20-23</sup> (Fig. 1). To strengthen magnetic interactions between the core ions, SMMs often have delocalized bonds, which can enhance their conducting properties. SMMs come in a variety of shapes and sizes and allow selective substitutions of the ligands to alter the coupling to the environment<sup>8,9,20,21,24</sup>. It is also possible to exchange the magnetic ions, thus changing the magnetic properties without modifying the structure or coupling<sup>25</sup>. Although grafting SMMs on surfaces has already led to important results, even more spectacular results will emerge from the rational design and tuning of SMM-based junctions.

From a physical viewpoint, SMMs combine the classical macroscale properties of a magnet to the quantum properties of a nanoscale entity. They offer crucial advantages over magnetic nanoparticles in that they are perfectly monodisperse and can be studied in crystals. They display an impressive array of quantum effects (Box 1), ranging from quantum tunnelling of the magnetization<sup>15,16</sup> to Berry-phase interference<sup>17</sup> and quantum coherence<sup>11</sup>, with important consequences for the physics of spintronic devices. Although the magnetic properties of SMMs can be affected when depositing on surfaces or between leads<sup>24</sup>, these systems remain a

Box 1 Dynamics of SMMs

SMMs are nanoscale magnetic molecules that exhibit slow relaxation of the magnetization at low temperatures<sup>8,9</sup>. They often crystallize into high-quality crystals, thus allowing for a structural determination and rationalization of their properties. The magnetic properties are described using a spin hamiltonian, which takes the form  $\hat{\mathcal{H}} = DS_z^2 + E(S_x^2 - S_y^2) + g\mu_B\mu_0\mathbf{S}\cdot\mathbf{H}$ , where  $S_x$ ,  $S_y$  and  $S_z$  are the spin components,  $D$  and  $E$  are the magnetic anisotropy constants, and the term  $g\mu_B\mu_0\mathbf{S}\cdot\mathbf{H}$  describes the Zeeman energy associated with an applied magnetic field  $\mathbf{H}$ . Excited spin states and higher-order anisotropy terms are neglected for simplicity. For SMMs,  $D < 0$  and an easy axis of magnetization is present along  $S_z$ . The energy potential takes the form of a double well, with the levels  $S_m = \pm S$  having the lowest energy and a potential barrier in between. To reverse the magnetization, the spin has to overcome a potential energy barrier  $\Delta = DS_z^2$  by climbing up and down all the  $(2S+1)$  energy levels (Fig. B1a). The relaxation time will thus follow a

thermally activated law, increasing exponentially as  $T$  is lowered. When the relaxation time is long at low temperatures, the system displays superparamagnetic behaviour with the opening of a hysteresis cycle (Fig. B1b).

Owing to their molecular nature, SMMs exhibit some striking quantum effects that affect the magnetization reversal mechanism. One of the most prominent is quantum tunnelling of the magnetization<sup>8,9,15–17</sup>. When  $\mathbf{H}$  is applied along  $z$ , levels with  $S_m < 0$  are shifted up and levels with  $S_m > 0$  are shifted down. Levels of positive and negative quantum numbers will then cross at  $\mathbf{H} = 0$  and at certain resonance fields. Transverse terms, containing  $S_x$  or  $S_y$ , turn the crossings into an avoided level-crossing and quantum tunnelling between the two wells can occur (Fig. B1a). The availability of this additional tunnelling mechanism for the relaxation of the magnetization produces the characteristic steps at the resonance fields in the hysteresis curve of SMMs (Fig. B1b).

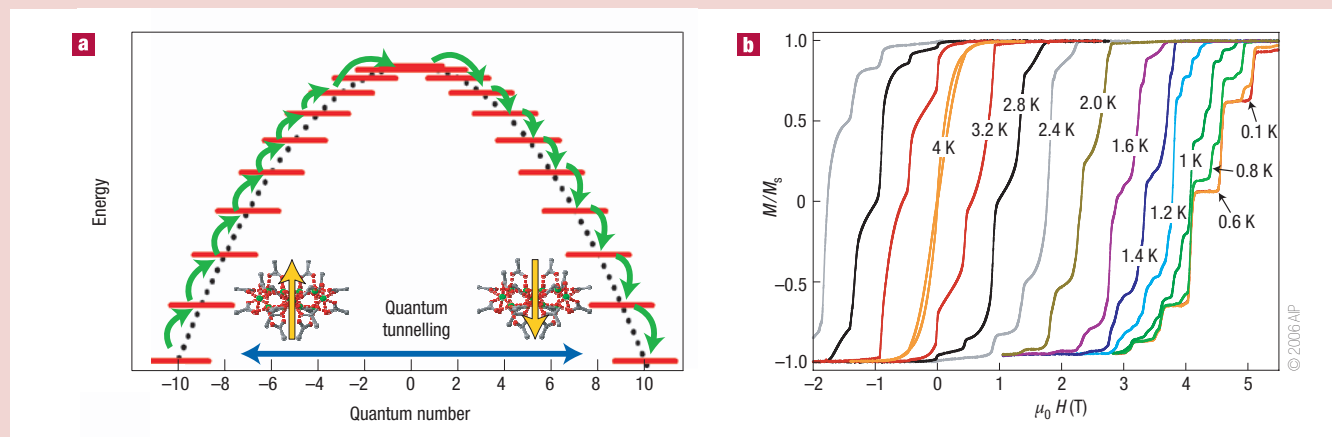


**Figure B1** Dynamics of the magnetization in SMMs. **a**, Schematic representation of the energy landscape of a SMM with a spin ground state  $S = 10$ . The magnetization reversal can occur via quantum tunnelling between energy levels (blue arrow) when the energy levels in the two wells are in resonance. Phonon absorption (green arrows) can also excite the spin up to the top of the potential energy barrier with the quantum number  $M = 0$ , and phonon emission descends the spin to the second well. **b**, Hysteresis loops of single crystals of  $[\text{Mn}_{12}\text{O}_{12}(\text{O}_2\text{CCH}_2\text{C}(\text{CH}_3)_2)_4(\text{CH}_3\text{OH})_4]$  SMM at different temperatures and a constant field sweep rate of  $2 \text{ mT s}^{-1}$  (data from ref. 65). The loops exhibit a series of steps, which are due to resonant quantum tunnelling between energy levels. As the temperature is lowered, there is a decrease in the transition rate due to reduced thermally assisted tunnelling. The hysteresis loops become temperature-independent below 0.6 K, demonstrating quantum tunnelling at the lowest energy levels.

step ahead of non-molecular nanoparticles, which have large size and anisotropy distributions.

MOLECULAR SPIN-TRANSISTOR

The first scheme we consider is a magnetic molecule attached between two non-magnetic electrodes. One possibility is to use a scanning tunnelling microscope (STM) tip as the first electrode and the conducting substrate as the second one (Fig. 2a). So far, only few atoms on surfaces have been probed in this way, revealing interesting Kondo effects<sup>26</sup> and single-atom magnetic anisotropies<sup>27</sup>. The next scientific step is to pass from atoms to molecules to observe richer physics and to modify the properties of the magnetic objects. Although isolated SMMs on gold have been obtained<sup>20–23</sup>, the rather drastic experimental requirements for studying them by STM — that is, very low temperatures and high magnetic fields — have not yet been achieved. The first theoretical work predicted that quantum tunnelling of the magnetization (Box 1) is detectable via the electric

current flowing through the molecule<sup>28</sup>, thus enabling the readout of the quantum dynamics of a single molecule.

Another possibility concerns break-junction devices<sup>29</sup>, which contain a gate electrode in addition to source and drain electrodes. Such a three-terminal transport device, called a molecular spin-transistor, is a single-electron transistor with non-magnetic electrodes and a single magnetic molecule as the island. The current passes through the magnetic molecule through the source and drain electrodes, and the electronic transport properties are tuned using a gate voltage  $V_g$  (Fig. 2b). Similarly to molecular electronics (Box 2), two experimental regimes can be distinguished, depending on the coupling between molecule and electrodes.

WEAK-COUPLING LIMIT

In the weak-coupling limit, charging effects dominate the transport. Transport takes place when a molecular orbital is in resonance with the Fermi energy  $E_F$  of the leads (Fig. B2), and electrons can then tunnel through the energy barrier into the molecular level and out

## Box 2 Molecular electronics

The energy spectrum of molecules and semiconducting quantum dots (QDs), are characterized by discrete electronic energy levels (Fig. B2). As much of the physics is the same whether a molecule or a QD is placed in the junction, the two are often used interchangeably. Although it is often complicated to know the spacing of all levels, many properties are determined by the energies of the highest occupied molecular orbital (HOMO) and the lowest unoccupied molecular orbital (LUMO).

Molecules can be weakly or strongly coupled to the electrodes, with low or high perturbations of molecular states by the presence of the electrodes (Fig. B2a–c). Physically, this is depicted by an energy barrier between the contacts and the molecule, whose height determines the mixing between the wavefunctions of the molecule and of the electrodes. When the energy broadening of the levels due to hybridization ( $\Gamma$ ) is smaller than the charging energy  $U$  of the molecule ( $\Gamma < U$ ), the molecule is weakly coupled to the leads, whereas for  $\Gamma > U$  strong coupling is obtained (Fig. B2a–c).

For  $\Gamma < U$  and at temperatures  $T$  comparable to the energy between the Fermi energy  $E_F$  of the leads and the HOMO or LUMO, electron transport occurs by emptying the HOMO or filling the LUMO. At low  $T$ , electron transport is blocked (Fig. B2d)

except for  $V_g$  values that bring the molecular levels in resonance with  $E_F$  (Fig. B2e) or for bias voltages that bring  $E_F$  to the energy of molecular levels (Fig. B2f). This regime, called Coulomb-blockade, leads to large regions of blocked conduction, forming characteristic Coulomb diamonds in differential conductance plots<sup>30,31</sup>. Vibrational and spin excitation levels can also lead to resonance levels and appear inside the diamonds, making transport measurements essentially a form of spectroscopy (Fig. B2g).

For  $\Gamma > U$ , the molecular wavefunctions are not appropriate eigenstates of the system, and are replaced by hybrid states. Hybridization shifts both the LUMO and HOMO closer to  $E_F$  and broadens the electronic states. Because electrons are delocalized between electrodes and the molecule, the system can be described by an occupancy fraction of the new HOMO and LUMO levels. When an unpaired electron occupies the HOMO, electrons moving to and from the molecule reverse the spin of the unpaired electron and a screening of the spin occurs, in analogy to the well-known Kondo effect<sup>37–40</sup>. Below a certain Kondo temperature  $T_K$ , the screening leads to a zero-bias conductance resonance, which is associated with the entangled state of electrons in the leads and in the molecule.

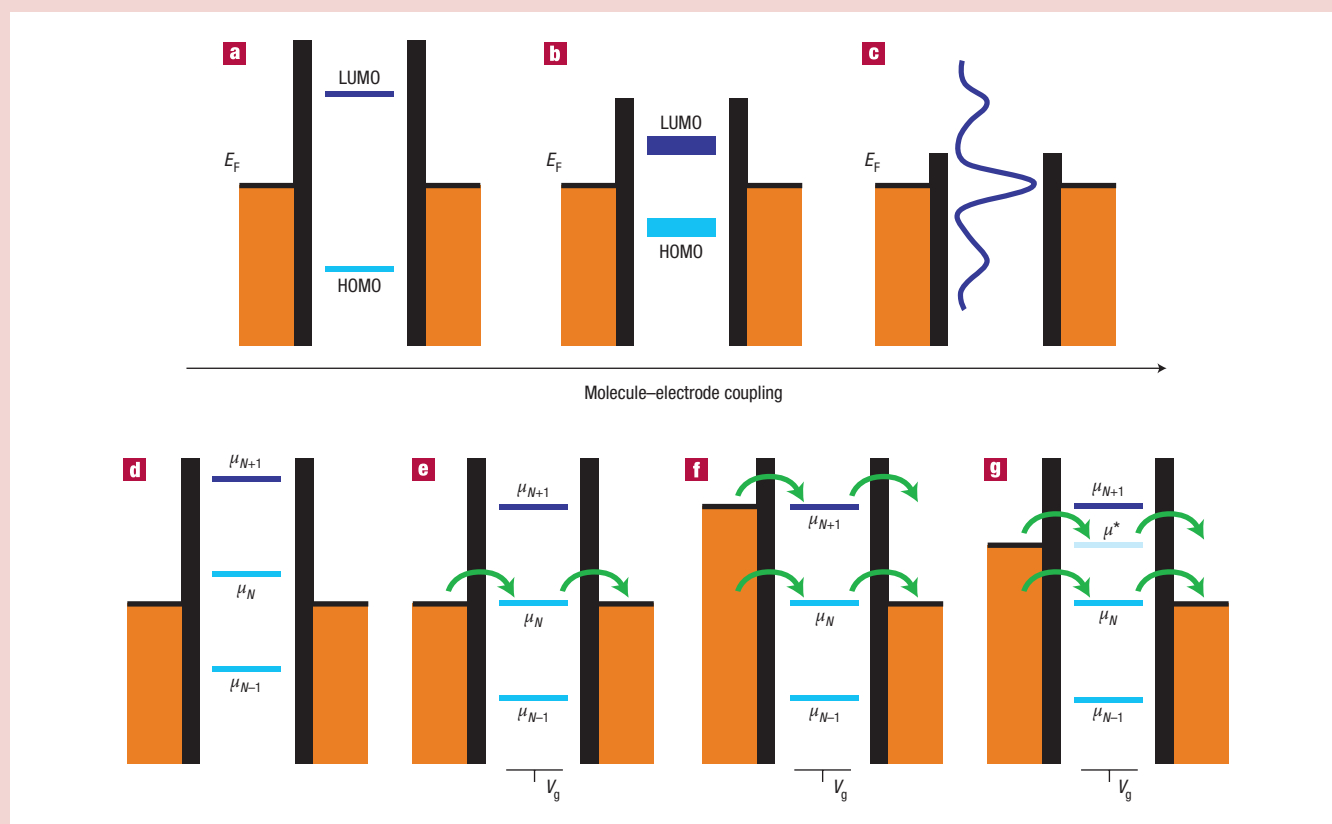


**Figure B2** Schematic representation of the basic processes of non-magnetic molecular electronics. **a–c**, Change of the molecular levels on varying the transparency of the tunnel barriers (black) between the electrodes and the molecule. The HOMO (light blue) and LUMO (dark blue) are well defined in the weak-coupling regime (**a**), become broader and closer to  $E_F$  as coupling is increased (**b**) and eventually give rise to a semicontinuous multi-peaked structure for very strong coupling (**c**). In this case, and when an unpaired spin characterizes the ground state of the QD, a screening of the spin occurs, in analogy to the well-known Kondo effect in solids containing magnetic impurities<sup>37–40</sup>. **d–g**, Processes giving rise to Coulomb diamonds;  $\mu_N$ ,  $\mu_{N-1}$  and  $\mu_{N+1}$  denote the electronic energy levels of the QD. Out of resonance (**d**) electrons cannot pass through the device. They can tunnel through the barrier only if the molecular levels are put in resonance with  $E_F$  using  $V_g$  (**e**). At higher bias voltage, two or more electronic levels (**f**) can contribute to the electron transport. Additional energy levels ( $\mu^*$ ; **g**), for example vibrational levels, excited electronic or nuclear spin levels, can also induce electronic transport through the QD.

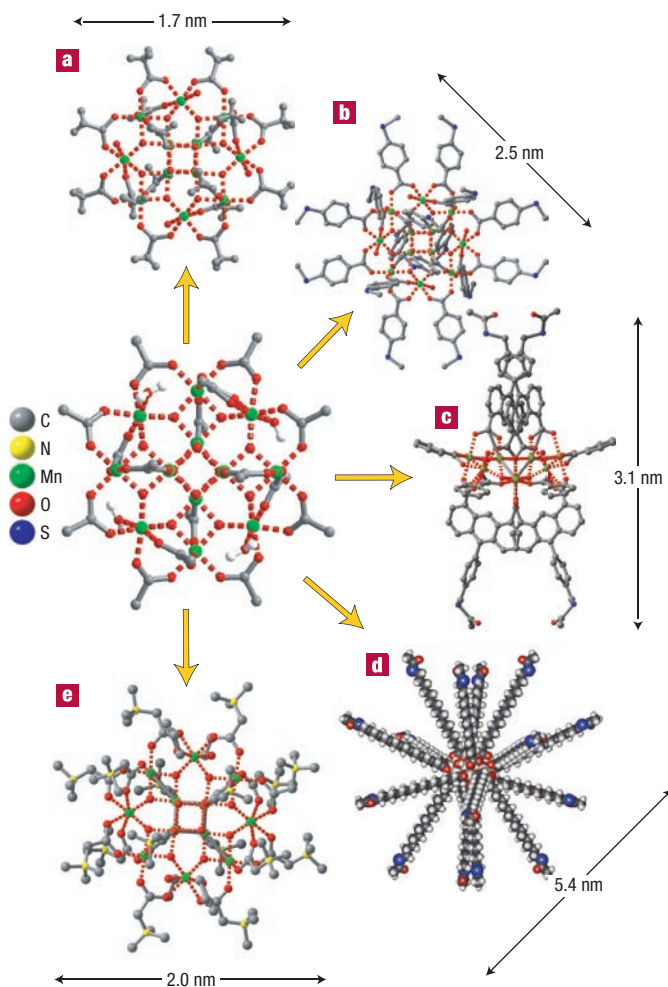


**Figure 1** Representative examples of the peripheral functionalization of the outer organic shell of the  $[\text{Mn}_{12}\text{O}_{12}(\text{CH}_3\text{COO})_{16}(\text{H}_2\text{O})_4]$  SMM (centre). Different functionalizations used to graft the SMM to surfaces are displayed: **a**,  $[\text{Mn}_{12}\text{O}_{12}(\text{C}(\text{CH}_3)_3\text{COO})_{16}(\text{H}_2\text{O})_4]$ . **b**,  $[\text{Mn}_{12}\text{O}_{12}(\rho\text{-CH}_3\text{-C}_6\text{H}_4\text{-COO})_{16}(\text{H}_2\text{O})_4]$ . **c**,  $[\text{Mn}_{12}\text{O}_{12}(\text{O}_2\text{CC}_6\text{H}_5)_8(1,8\text{-dicarboxyl-10-(4-acetylsulphanylmethyl-phenyl)-anthracene-1,8-dicarboxylic acid})_4(\text{H}_2\text{O})_4]$ . **d**,  $[\text{Mn}_{12}\text{O}_{12}(\text{CH}_3\text{OS}(\text{CH}_2)_{15}\text{COO})_{16}(\text{H}_2\text{O})_4]$ . **e**,  $[\text{Mn}_{12}\text{O}_{12}((\text{CH}_3)_3\text{NCH}_2\text{COO})_{16}(\text{H}_2\text{O})_4]^{16+}$ . All structures are determined by X-ray crystallography, except **d**, which is a model structure. Solvent molecules have been omitted.

into the drain electrode. The resonance condition is obtained by shifting the energy levels with  $V_g$  and Coulomb-blockade diamonds appear in differential conductivity maps as a function of source–drain voltage and  $V_g$  (ref. 30).

The experimental realization of this scheme has been achieved by substituting the acetate molecules of the  $[\text{Mn}_{12}\text{O}_{12}(\text{CH}_3\text{COO})_{16}(\text{H}_2\text{O})_4]$  SMM with thiol-containing ligands (Fig. 1), which bind the SMM to the gold electrodes with strong and reliable covalent bonds<sup>18</sup>. An alternative route is to use short but weak binding ligands<sup>19</sup>: in both cases the peripheral groups act as tunnel barriers and help conserve the magnetic properties of the SMM in the junction. As the electron transfer involves the charging of the molecule, we must consider, in addition to the neutral state, the magnetic properties of the negatively and positively charged species. This introduces an important difference with respect to the homologous measurements on diamagnetic molecules, where the assumption is often made that charging of the

molecule does not significantly alter the internal degrees of freedom<sup>31</sup>. Because crystals of the charged species can be obtained, SMMs permit direct comparison between spectroscopic transport measurements and more traditional characterization methods. In particular, magnetization measurements, electron paramagnetic resonance, and neutron spectroscopy can provide energy-level spacings and anisotropy parameters<sup>8,9</sup>. In the case of the  $[\text{Mn}_{12}\text{O}_{12}(\text{CH}_3\text{COO})_{16}(\text{H}_2\text{O})_4]$  SMM, positively charged clusters possess a lower anisotropy barrier<sup>32</sup>. As revealed by the first Coulomb-blockade measurements, the presence of these states is fundamental for explaining transport through the clusters<sup>18,19</sup>. Negative differential conductance was found that might be due to the magnetic characteristics of SMMs.

Studies in magnetic fields showed the first evidence of spin-transistor properties<sup>19</sup>. Degeneracy at zero field and nonlinear behaviour of the excitations as a function of field are typical of tunnelling via a magnetic molecule. In these first studies, the lack of a hysteretic response can be due, besides environmental effects<sup>24</sup>, to the alternation of the molecules during the grafting procedure, to the population of excited states with lower energy barriers, or it might also be induced by the source–drain voltage scan performed at each field value.

Theoretical investigations in the weak-coupling regime predict many interesting effects. For example, a direct link between shot noise measurements and the detailed microscopic magnetic structure of SMMs has been proposed<sup>33</sup>, allowing the connection of structural and magnetic parameters to the transport features and therefore a characterization of SMMs using transport measurements. This opens the way to rational design of SMMs for spintronics, and to test the physical properties of related compounds. The first step in this direction has already been made by comparing the expected response of chemically related SMMs<sup>34</sup>. Note that this direct link cannot be established for nanoparticles or quantum-dots (QDs) because they do not possess a unique chemical structure.

A complete theoretical analysis as a function of the angle between the easy axis of magnetization and the magnetic field showed that the response persists whatever the orientation of the SMM in the junction, and that even films of SMMs should retain many salient properties of single-molecule devices<sup>35,36</sup>.

#### STRONG-COUPLING LIMIT

For strong electronic coupling between the molecule and the leads, higher-order tunnel processes become important, leading to the Kondo effect<sup>37–40</sup> (Box 2). This regime has been attained using paramagnetic molecules containing one<sup>41</sup> or two magnetic centres<sup>42</sup>, but remains elusive for SMMs.

The first mononuclear magnetic molecule investigated (Fig. 2c) is a Co(II) ion bound by two terpyridine ligands, TerPy, attached to the electrodes with chemical groups of variable length<sup>41</sup>. The system with the longer alkyl spacer, due to a lower transparency of the barrier, displays Coulomb-blockade diamonds, which are characteristic for the weak-coupling regime, but no Kondo peak. Experiments conducted as a function of magnetic field reveal the presence of excited states related to spin excitations, in agreement with the effective spin  $S = 1/2$  state usually attributed to  $\text{Co}^{2+}$  ions at low temperatures. However, a Landé factor  $g = 2.1$  is found, which is unexpected for  $\text{Co}^{2+}$  ions having strong spin-orbit coupling and high magnetic anisotropy — this point therefore needs further investigation. The same complex with the thiol directly connected to the TerPy ligand (Fig. 2d) shows strong coupling to the electrodes, with exceptionally high Kondo temperatures of around 25 K (ref. 41).

Additional physical effects of considerable interest were obtained using a simple molecule containing two magnetic centres<sup>42</sup>. This molecule, the divanadium molecule  $[(N,N',N''\text{-trimethyl-1,4,7-triazacyclononane})_2\text{V}_2(\text{CN})_4(\mu\text{-C}_4\text{N}_4)]$  (Fig. 2e) was directly grafted to the electrodes, so as to have the highest possible transparency<sup>42</sup>. The

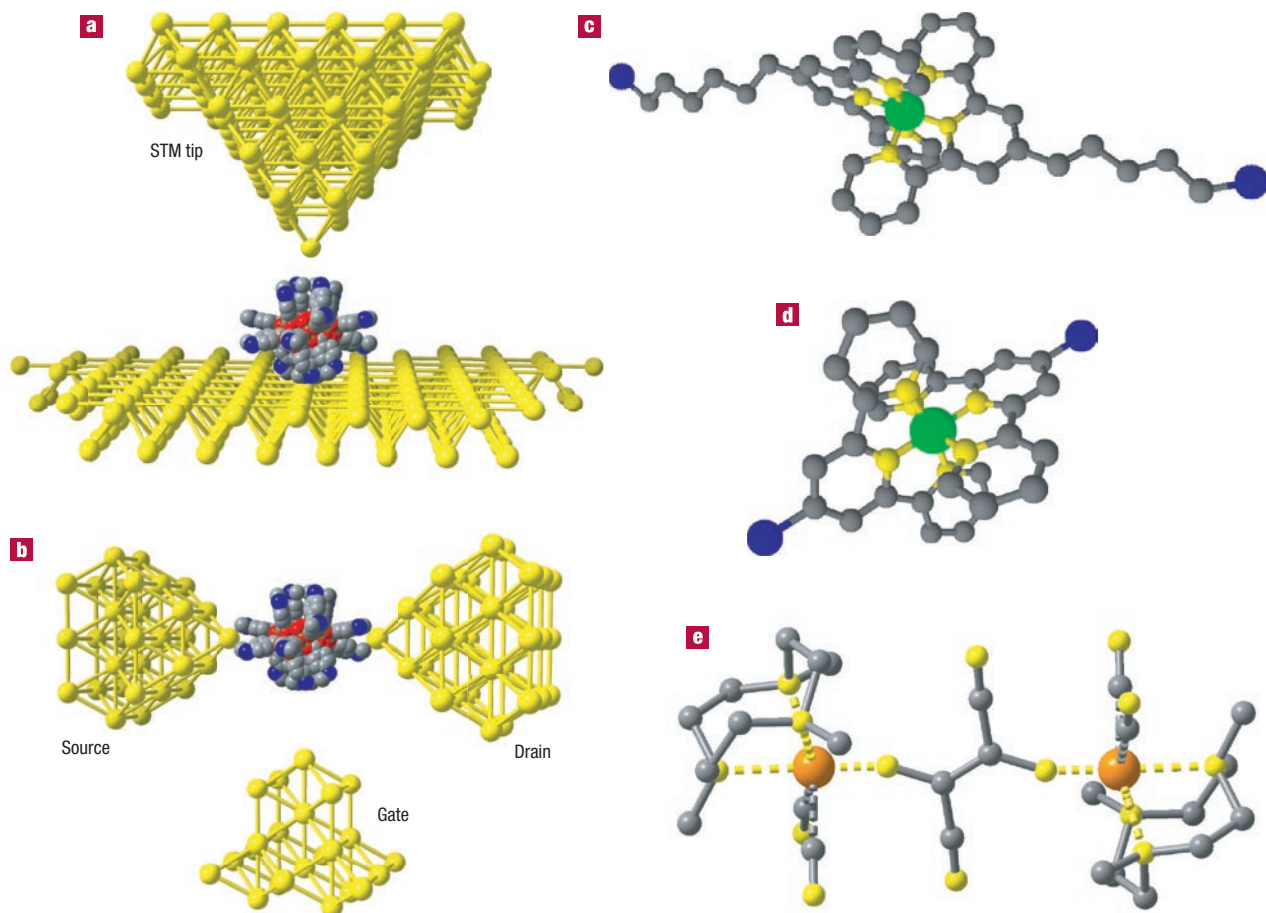


**Figure 2** Transport experiments on SMMs. **a**, Schematic showing the use of an STM tip to perform transport experiments on surface-grafted SMMs. **b**, Schematic of SMM-based molecular transistors, in which a gate voltage can modulate transport. **c**, [Co(TerPy)<sub>2</sub>] mononuclear magnet molecule with alkyl spacers, permitting transport in the weakly coupled regime<sup>41</sup>. **d**, [Co(TerPy)<sub>2</sub>] without spacers, showing strong coupling and the Kondo effect<sup>41</sup>. **e**, Divanadium [(*N,N',N''*-trimethyl-1,4,7-triazacyclononane)<sub>2</sub>V<sub>2</sub>(CN)<sub>4</sub>(μ-C<sub>4</sub>N<sub>4</sub>)] molecular magnet showing the Kondo effect only in the charged state<sup>42</sup>. The colour code is the same as for Fig. 1, except for Co atoms (green) and V atoms (orange).

molecule can be tuned, using  $V_g$ , into two differently charged states. The neutral state, due to antiferromagnetic coupling between the two magnetic centres, has  $S = 0$ , whereas the positively charged state has  $S = 1/2$ . Kondo features are found, as expected<sup>37–40</sup>, only for the state in which the molecule has a non-zero spin moment. This nicely demonstrates that magnetic molecules with multiple centres and antiferromagnetic interactions enable the Kondo effect to be switched on and off, depending on their charge state. The Kondo temperature is again exceptionally high, exceeding 30 K, and its characterization as a function of  $V_g$  indicates that not only spin but also orbital degrees of freedom have an important role in the Kondo resonance of single molecules. Molecular magnets, in which spin–orbit interaction can be tuned without altering the structure<sup>9,25</sup>, are appealing for investigating this physics further.

The Kondo temperatures observed in the two cases<sup>41,42</sup> are much higher than those obtained for QDs and carbon nanotubes<sup>37–40</sup>, and are extremely encouraging. The study of the superparamagnetic transition of SMMs while in the Kondo regime thus seems achievable, possibly leading to an interesting interplay of the two effects. To observe the Kondo regime one might start with small SMMs<sup>25,43</sup>, with core states more affected by the proximity of the leads, and use short and strongly bridging ligands to connect SMMs to the electrodes<sup>20,41</sup>.

Theoretical investigations have explored the rich physics of this regime<sup>44,45</sup>, revealing that the Kondo effect should even be visible in

SMMs with  $S > 1/2$  (ref. 45). This is in contrast to expectations for a system with an anisotropy barrier, where the blocked spin should hinder co-tunnelling processes. However in SMMs, the presence of a transverse anisotropy induces a Kondo resonance peak<sup>45</sup>. The observation of this new physical phenomenon should be possible because of the tunability of SMMs, allowing a rational choice of the physical parameters governing the tunnelling process: low-symmetry transverse terms are particularly useful, because selection rules apply for high-symmetry terms.

The first theoretical predictions argued that the Kondo effect should be present only for half-integer spin molecules. However, the particular quantum properties of SMMs allow the Kondo effect to occur even for integer spins. In addition, the presence of the so-called Berry-phase interference<sup>17</sup>, a geometrical quantum-phase effect, can produce not only one Kondo resonance peak, but a series of peaks as a function of applied magnetic field<sup>46</sup>. These predictions demonstrate how the molecular nature of SMMs and the quantum effects they exhibit differentiate them from inorganic QDs and nanoparticles, and should permit the observation of otherwise prohibited phenomena.

#### MOLECULAR SPIN-VALVE

A molecular spin-valve (SV)<sup>7</sup> is similar to a spin transistor but contains at least two magnetic elements (Fig. 3a,b). SVs change

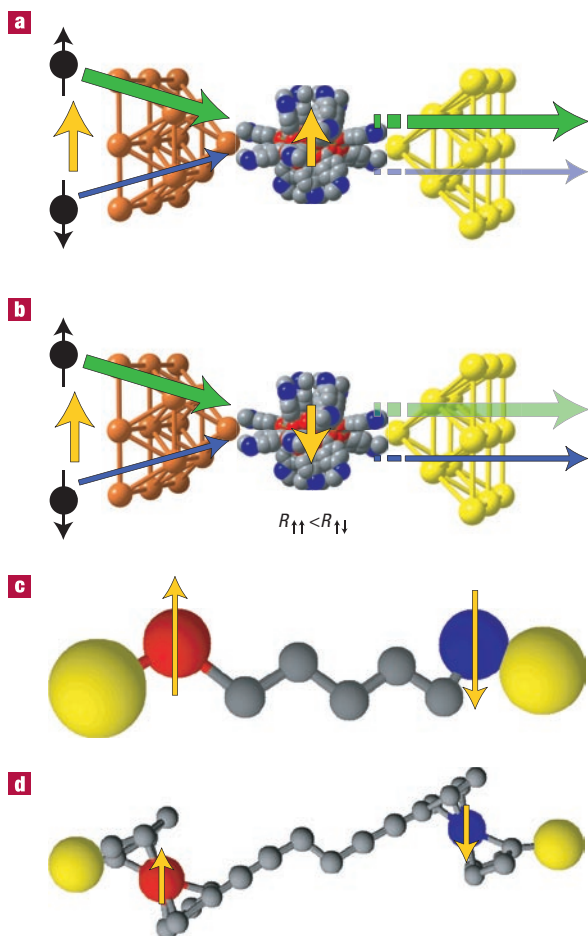


**Figure 3** Spin valves based on molecular magnets. Yellow arrows represent the magnetization direction. **a**, Parallel configuration of the magnetic source electrode (orange) and molecular magnetization, with diamagnetic drain electrode (yellow). Spin-up majority carriers (thick green arrow) are not affected by the molecular magnetization, whereas the spin-down minority carriers (thin blue arrow) are partially reflected back. **b**, Antiparallel configuration: majority spin-up electrons are only partially transmitted by the differently polarized molecule, whereas the minority spin-down electrons pass unaffected. Assuming that the spin-up contribution to the current is larger in the magnetic contact, this configuration has higher resistance than that of the previous case. **c**, Theoretical schematic of a spin-valve configuration with non-magnetic metal electrodes<sup>7</sup> and **d**, proposed molecular magnet [(C<sub>5</sub>H<sub>5</sub>)Co(C<sub>5</sub>H<sub>4</sub>-CCCH<sub>2</sub>CH<sub>2</sub>CC-C<sub>5</sub>H<sub>4</sub>)Fe(C<sub>5</sub>H<sub>5</sub>)] between gold electrodes: a conjugated molecule bridges the cobaltocene (red) and ferrocene (blue) moieties<sup>51</sup>.

their electrical resistance for different mutual alignments of the magnetizations of the electrodes and of the molecule, analogous to a polarizer–analyser set-up. Non-molecular devices are already used in hard-disk drives, owing to the giant- and tunnel-magnetoresistance effects. Good efficiency has already been demonstrated for organic materials<sup>4</sup>, molecular SVs are therefore actively sought after<sup>47,48</sup>. As only few examples of molecular SVs exist<sup>49,50</sup>, the fundamental physics behind these devices remains largely unexplored, and is likely to be the focus of considerable attention in the near future. The simplest SV consists of a diamagnetic molecule in between two magnetic leads, which can be metallic or semiconducting. The first experiments sandwiched a C<sub>60</sub> fullerene between Ni electrodes, and exhibited a very large negative magnetoresistance effect<sup>49</sup>. Another interesting possibility is to use carbon nanotubes connected with

magnetic half-metallic electrodes transforming spin information into large electrical signals<sup>50</sup>.

A SMM-based SV can have one or two magnetic electrodes (Fig. 3a,b), or the molecule can possess two magnetic centres in between two non-magnetic leads (Fig. 3c,d), in a scheme reminiscent of early theoretical models of SVs<sup>7</sup>. Molecules with two magnetic centres connected by a molecular spacer are well known in molecular magnetism, and a double-metallocene junction has been studied theoretically<sup>51</sup>. This seems a good choice, as the metallocenes leave the *d*-electrons of the metals largely unperturbed.

Theory indicates that, when using SMMs, the contemporary presence, at high bias, of large currents and slow relaxation will form a physically interesting regime<sup>52,53</sup>. Only spins parallel to the molecular magnetization can flow through the SMM and the current will display, for a time equivalent to the relaxation time, a very high spin polarization. For large currents this process can lead to a selective drain of spins with one orientation from the source electrode, thus transferring a large amount of magnetic moment from one lead to the other. This phenomenon, due to a sole SMM, has been named giant spin amplification<sup>52</sup>, and offers a convenient way to read the magnetic state of the molecule. The switching of the device seems more complicated, at first sight, involving a two-step process that includes the application of a magnetic field and the variation of the bias voltage. However, it has recently been suggested that the spin-polarized current itself can be sufficient to switch the magnetization of a SMM<sup>54</sup>. The switching can be detected in the current as a step if both leads are magnetic and have parallel magnetization, or as a sharp peak for the antiparallel configuration.

#### MOLECULAR MULTIDOT DEVICES

Even more interesting phenomena can be obtained by transport measurements through a controlled number of molecules or multiple centres inside the same molecule<sup>55</sup>. The double-metallocene molecule<sup>51</sup> (Fig. 3d) can already be considered as a multidot system with level crossings giving rise to negative differential conductance<sup>51</sup>. The possibilities offered by the chemistry of SMMs seem particularly promising here<sup>11,56,57</sup>. Only one experiment, up to now, has considered the chemical fabrication of multidot devices<sup>58</sup>, obtaining a controlled sequence of CdSe QDs connected by *p*-benzenedithiol molecular bridges (Fig. 4a), in a process reminiscent of the solid-phase synthesis of peptides<sup>59</sup>. Ultrafast pump–probe magneto-optical experiments, probing the spin transfer through the  $\pi$ -conjugated molecular bridge, indicate that the process is coherent and that the bridging molecule acts as a quantum-information bus. Coupled SMMs or spin-transfer molecular compounds<sup>56,57</sup> use similar molecular bridges, and we can thus expect analogous performances for spin transfer in bridged SMMs. With small decoherence<sup>11–14</sup>, this should open the way to solid-state quantum computation protocols.

A simpler situation concerns a double-dot (Fig. 4b) with three terminals, where the current passes through a non-magnetic quantum conductor (quantum wire, nanotube, molecule or QD). The magnetic molecule is only weakly coupled to the non-magnetic conductor but its spin can influence the transport properties, permitting readout of the spin state with minimal back-action. Several mechanisms can be exploited to couple the two systems. One appealing way is to use a carbon nanotube as a detector of the magnetic flux variation, possibly using a nanoSQUID<sup>60</sup>. Another possibility involves the indirect detection of the spin state through electrometry. Indeed, a non-magnetic quantum conductor at low temperatures behaves as a QD for which charging processes become quantized, giving rise to Coulomb blockade and the Kondo effect depending on the coupling to the leads (Box 2). Any slight change in the electrostatic environment (controlled by the gate) can induce a shift of the Coulomb diamonds of the device, leading to a conductivity variation of the QD at constant

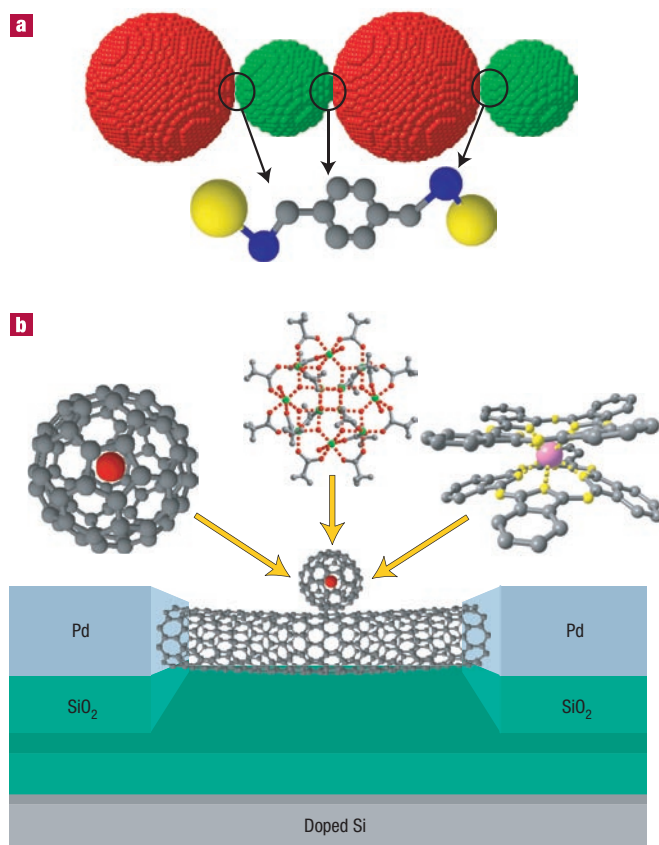


**Figure 4** Multidot devices. **a**, Chemically bridged multi-QDs forming chains in which coherent spin transfer can be achieved and followed optically. The  $p\text{-C}_6\text{H}_4\text{-(CH}_2\text{SH)}_2$  molecule, depicted below the chain, bridges the inorganic QDs and acts as a molecular buffer. **b**, Magnetic molecules proposed for grafting on suspended carbon nanotubes connected to Pd electrodes (from left to right): a C<sub>60</sub> fullerene including a rare-earth atom<sup>64</sup>, the [Mn<sub>12</sub>O<sub>12</sub>(C(CH<sub>3</sub>)<sub>3</sub>COO)<sub>16</sub>(H<sub>2</sub>O)<sub>4</sub>] SMM<sup>20</sup> and the rare-earth-based double-decker [Tb(phtalocyanine)<sub>2</sub>] SMM<sup>25</sup>. The gate voltage of the double-dot device is obtained by a doped Si substrate covered by a SiO<sub>2</sub> insulating layer.

$V_g$ . QDs are therefore accurate electrometers. When the QD is coupled, even weakly, with a magnetic object, owing to the Zeeman energy the spin flip at non-zero field induces a change of the electrostatic environment of the QD. This ‘magneto-Coulomb’ effect<sup>61</sup>, enables detection of the magnetization reversal of the molecule.

Other routes of multidot devices use weak exchange or dipole coupling between the magnetic molecule and the QD<sup>56</sup>. It is interesting to probe these effects as a function of the number of trapped electrons, because odd or even numbers of electrons should lead to different couplings.

The main advantage of these double-dot devices is that the weak coupling between the SMM and the quantum conductor ensures preservation of the intrinsic properties of the SMM. Because coupling is small, these devices will enable non-destructive readout of the spin states.

## OUTLOOK

In conclusion, SMM-based molecular spintronics is an emerging field full of fascinating challenges for theoreticians, experimental physicists and chemists alike. These devices are exciting experimental playgrounds for testing quantum effects at the single-molecule level.

The unique properties of SMMs will soon lead to the design of molecules for specific transport characteristics using the flexibility of supramolecular chemistry.

SMM-based systems might not find their way into everyday electronics, because of their low operational temperatures. However, modulating the response of spintronic devices using quantum effects, besides its fundamental importance, can lead to important consequences for applications. As molecular-based storage devices are becoming feasible<sup>62</sup>, SMMs offer the possibility to magnetically store information at a molecular level. The absence of conformational changes that usually destroy coherence, as in molecular machines<sup>62</sup>, makes the development of SMM-based quantum computation devices possible. This is particularly true when considering that the coherence time of SMMs is extremely long, compared with that of metallic and semiconducting materials. Another important advantage of molecular spintronics is the weak spin-orbit and hyperfine interactions of organic molecules, which help preserve electron-spin polarization over a much greater distance than in conventional semiconductor systems. Because a spin-polarized current, passing through a SMM, should allow the reading and reversing of its magnetization, such devices can be a breakthrough for quantum information processing. Last but not least, specific functions (for example, switchability with light, electric field and so on) could be directly integrated into the molecule.

In the perspective of molecular spintronics, some new SMMs look most promising. Rare-earth-based double-decker molecules, for example, offer a family of isostructural SMMs with tunable anisotropy<sup>25</sup>. The conjugated structure of the porphyrine ligands is particularly suitable for electron transport and, owing to their symmetric disposition around the rare-earth element, the relevant magnetic parameters can be calculated or extracted from electron paramagnetic resonance and optical data<sup>24</sup>. Because these systems have very strong couplings between electron and nuclear spins, they exhibit exotic characteristics that can be used as fingerprints of the presence of the molecule in the junctions or on the nanotubes<sup>63</sup>. Magnetic atoms imprisoned inside fullerenes<sup>64</sup> also look very attractive. They offer a clean environment around an otherwise isolated atom that can be nicely modelled and compared to transport measurements of empty fullerenes<sup>49</sup>. Finally, we would like to mention that there is a vast amount of trivial-looking magnetic molecules in the chemistry literature, which represent a precious unexploited resource for molecular spintronics.

doi:10.1038/nmat2133

## References

- Wolf, S. A. *et al.* Spintronics: a spin-based electronics vision for the future. *Science* **294**, 1488–1495 (2001).
- Awshalom, D. D. & Flatté, M. M. Challenges for semiconductor spintronics. *Nature Phys.* **3**, 153–159 (2007).
- Dery, H., Dalal, P., Cywiński, Ł. & Sham, L. J. Spin-based logic in semiconductors for reconfigurable large-scale circuits. *Nature* **447**, 573–576 (2007).
- Xiong, Z. H., Wu, D., Vally Vardeny, Z. & Shi, J. Giant magnetoresistance in organic spin-valves. *Nature* **427**, 821–824 (2004).
- Ratner, M. A. (ed.) Special feature on molecular electronics. *Proc. Natl Acad. Sci.* **102**, 8800–8837 (2005).
- Tao, N. J. Electron transport in molecular junctions. *Nature Nanotech.* **1**, 173–181 (2006).
- Sanvito, S. & Rocha, A. R. Molecular spintronics: The art of driving spin through molecules. *J. Comput. Theor. Nanosci.* **3**, 624–642 (2006).
- Christou, G., Gatteschi, D., Hendrickson, D. N. & Sessoli, R. *Mater. Res. Soc. Bull.* **25**, 66–71 (2000).
- Gatteschi, D., Sessoli, R. & Villain, J. *Molecular Nanomagnets* (Oxford Univ. Press, New York, 2007).
- Carretta, S. *et al.* Quantum oscillations of the total spin in a heterometallic antiferromagnetic ring: Evidence from neutron spectroscopy. *Phys. Rev. Lett.* **98**, 167401 (2007).
- Ardavan, A. *et al.* Will spin-relaxation times in molecular magnets permit quantum information processing? *Phys. Rev. Lett.* **98**, 057201 (2007).
- Leunenberger, M. N. & Loss, D. Quantum computing in molecular magnets. *Nature* **410**, 789–793 (2001).
- Troiani, F. *et al.* Molecular engineering of antiferromagnetic rings for quantum computation. *Phys. Rev. Lett.* **94**, 207208 (2005).
- Lehmann, J., Gaita-Ariño, A., Coronado, E. & Loss, D. Spin qubits with electrically gated polyoxometalate molecules. *Nature Nanotech.* **2**, 312–317 (2007).

15. Friedman, J. R., Sarachik, M. P., Tejada, J. & Ziolo, R. Macroscopic measurement of resonant magnetization tunneling in high-spin molecules. *Phys. Rev. Lett.* **76**, 3830 (1996).
16. Thomas, L. *et al.* Macroscopic quantum tunnelling of magnetization in a single crystal of nanomagnets. *Nature* **383**, 145–147 (1996).
17. Wernsdorfer, W. & Sessoli, R. Quantum phase interference and parity effects in magnetic molecular clusters. *Science* **284**, 133–135 (1999).
18. Heersche, H. B. *et al.* Electron transport through single Mn<sub>12</sub> molecular magnets. *Phys. Rev. Lett.* **96**, 206801 (2006).
19. Jo, M.-H. *et al.* Signatures of molecular magnetism in single-molecule transport spectroscopy. *Nano. Lett.* **6**, 2014–2020 (2006).
20. Cornia, A. *et al.* Preparation of novel materials using SMMs. *Struct. Bond.* **122**, 133–161 (2006).
21. Fleury, B. *et al.* a new approach to grafting a monolayer of oriented Mn12 nanomagnets on silicon. *Chem. Comm.* 2020–2022 (2005).
22. Naitabdi, A., Bucher, J.-P., Gerber, Ph., Rabu, P. & Drillon, M. Self-assembly and magnetism of Mn<sub>12</sub> nanomagnets on native and functionalized gold surfaces. *Adv. Mater.* **17**, 1612–1616 (2005).
23. Coronado, E. *et al.* Polycationic Mn<sub>12</sub> single-molecule magnets as electron reservoirs with S>10 ground states. *Angew. Chem. Int. Ed.* **43**, 6152–6156 (2004).
24. Bogani, L. *et al.* Magneto-optical investigations of nanostructured materials based on single-molecule magnets monitor strong environmental effects. *Adv. Mater.* **19**, 3906–3911 (2007).
25. Ishikawa, N., Sugita, M., Ishikawa, T., Koshihara, S. & Kaizu, Y. Mononuclear lanthanide complexes with a long magnetization relaxation time at high temperatures: A new category of magnets at the single-molecular level. *J. Phys. Chem. B* **108**, 11265–11271 (2004).
26. Wahl, P. *et al.* Exchange interaction between single magnetic adatoms. *Phys. Rev. Lett.* **98**, 056601 (2007).
27. Hirjibehedin, C. F. *et al.* Large magnetic anisotropy of a single atomic spin embedded in a surface molecular network. *Science* **317**, 1199–1202 (2007).
28. Kim, G.-H. & Kim, T.-S. Electronic transport in single molecule magnets on metallic surfaces. *Phys. Rev. Lett.* **92**, 137203 (2004).
29. Park, H., Kim, A. K. L., Alivisatos, A. P., Park J. & McEuen, P. L. Fabrication of metallic electrodes with nanometer separation by electromigration. *Appl. Phys. Lett.* **75**, 301–303 (1999).
30. Hanson, R., Kouwenhoven, L. P., Petta, J. R., Tarucha S. & Vandersypen L. M. K. Spins in few-electron quantum dots. *Rev. Mod. Phys.* **79**, 1217–1265 (2007).
31. Kouwenhoven, L. P. *et al.* in *Mesoscopic Electron Transport* (eds Sohn, L. L., Kouwenhoven, L. P. & Schön, G.) 105–214 (Series E 345, Kluwer, 1997).
32. Chakov, N. E., Soler, M., Wernsdorfer, W., Asbboud, K. A. & Christou, G. Single-molecule magnets: Structural characterization, magnetic properties, and <sup>19</sup>F NMR spectroscopy of a Mn<sub>12</sub> family spanning three oxidation levels. *Inorg. Chem.* **44**, 5304–5321 (2005).
33. Romeike, C., Wegewijs, M. R. & Schoeller, H. Spin quantum tunneling in single molecule magnets: Fingerprints in transport spectroscopy of current and noise. *Phys. Rev. Lett.* **96**, 196805 (2006).
34. Romeike, C. *et al.* Charge-switchable molecular nanomagnet and spin-blockade tunneling. *Phys. Rev. B* **75**, 064404 (2007).
35. Erste, F. & Timm, C. Cotunneling and nonequilibrium magnetization in magnetic molecular monolayers. *Phys. Rev. B* **75**, 195341 (2007).
36. Timm, C. Tunneling through magnetic molecules with arbitrary angle between easy axis and magnetic field. *Phys. Rev. B* **76**, 014421 (2007).
37. Goldhaber-Gordon, D. *et al.* Kondo effect in a single-electron transistor. *Nature* **391**, 156–159 (1998).
38. Cronenwett, S. M., Oosterkamp, T. H. & Kouwenhoven, L. P. A tunable Kondo effect in quantum dots. *Science* **281**, 540–544 (1998).
39. van der Wiel, W. G. *et al.* The Kondo effect in the unitary limit. *Science* **289**, 2105–2108 (2000).
40. Nygard, J., Cobden, D. H. & Lindelof, P. E. Kondo physics in carbon nanotubes. *Nature* **408**, 342–346 (2000).
41. Park, J. *et al.* Coulomb blockade and the Kondo effect in single-atom transistors. *Nature* **417**, 722–725 (2002).
42. Liang, W., Shores, M. P., Bockrath, M. & Long, J. R. Kondo resonance in a single-molecule transistor. *Nature* **417**, 725–729 (2002).
43. Aromi, G. & Brechin, E. K. Synthesis of 3d metallic single-molecule magnets. *Struct. Bond.* **122**, 1–67 (2006).
44. Romeike, C., Wegewijs, M. R., Hofstetter W. & Schoeller, H. Kondo-transport spectroscopy of single molecule magnets. *Phys. Rev. Lett.* **97**, 206601 (2006).
45. Romeike, C., Wegewijs, M. R., Hofstetter, W. & Schoeller, H. Quantum-tunneling-induced kondo effect in single molecular magnets. *Phys. Rev. Lett.* **96**, 196601 (2006).
46. Leuenberger, M. N. & Mucciolo, E. R. Berry-phase oscillations of the Kondo effect in single-molecule magnets. *Phys. Rev. Lett.* **97**, 126601 (2006).
47. Waldron, D., Haney, P., Larade, B., MacDonald, A. & Guo, H. Nonlinear spin current and magnetoresistance of molecular tunnel junctions. *Phys. Rev. Lett.* **96**, 166804 (2006).
48. Rocha, A. R. *et al.* Towards molecular spintronics. *Nature Mater.* **4**, 335–339 (2005).
49. Pasupathy, A. N. *et al.* The Kondo effect in the presence of ferromagnetism. *Science* **306**, 86–89 (2004).
50. Hueso L. E. *et al.* Transformation of spin information into large electrical signals using carbon nanotubes. *Nature* **445**, 410–413 (2007).
51. Liu, R., Ke, S.-H., Baranger, H. U. & Yang, W. Negative differential resistance and hysteresis through an organometallic molecule from molecular-level crossing. *J. Am. Chem. Soc.* **128**, 6274–6275 (2006).
52. Timm, C. & Elste, F. Spin amplification, reading, and writing in transport through anisotropic magnetic molecules. *Phys. Rev. B* **73**, 235304 (2006).
53. Elste, F. & Timm, C. Transport through anisotropic magnetic molecules with partially ferromagnetic leads: Spin-charge conversion and negative differential conductance. *Phys. Rev. B* **73**, 235305 (2006).
54. Misiorny, M. & Barnaś, J. Magnetic switching of a single molecular magnet due to spin-polarized current. *Phys. Rev. B* **75**, 134425 (2007).
55. van der Wiel, W. G. *et al.* Electron transport through double quantum dots. *Rev. Mod. Phys.* **75**, 1–22 (2003).
56. Wernsdorfer, W., Aliaga-Alcalde, N., Hendrickson, D. N. & Christou G. Exchange-biased quantum tunneling in a supramolecular dimer of single-molecule magnets. *Nature* **416**, 406–409 (2002).
57. Affronte, M. *et al.* Linking rings through diamines and clusters: Exploring synthetic methods for making magnetic quantum gates. *Angew. Chem. Int. Ed.* **44**, 6496–6490 (2005).
58. Ouyang, M. & Awschalom, D. Coherent Spin-transfer between molecularly bridged quantum dots. *Science* **301**, 1074–1076 (2003).
59. Merrifield, B. *Solid Phase Synthesis* Available at <[http://nobelprize.org/nobel\\_prizes/chemistry/laureates/1984/merrifield-lecture.html](http://nobelprize.org/nobel_prizes/chemistry/laureates/1984/merrifield-lecture.html)>.
60. Cleuziou, J.-P., Wernsdorfer, W., Bouchiat, V., Ondarçuhu, T. & Monthieux, M. Carbon nanotube superconducting quantum interference device. *Nature Nanotech.* **1**, 53–59 (2006).
61. Shimada, H., Ono, K. & Otuka, Y. Driving the single-electron device with a magnetic field. *J. Appl. Phys.* **93**, 8259–8264 (2003).
62. Green, J. E. *et al.* A 160-kilobit molecular electronic memory patterned at 10<sup>11</sup> bits per square centimeter. *Nature* **445**, 414–418 (2007).
63. Ishikawa, N., Sugita, M. & Wernsdorfer, W. Quantum tunneling of magnetization in lanthanide single-molecule magnets: Bis(phthalocyaninato)terbium and bis(phthalocyaninato)dysprosium anions. *Angew. Chem. Int. Ed.* **44**, 2931–2935 (2005).
64. Kasumov, A. *et al.* Proximity effect in a superconductor-metallofullerene-superconductor molecular junction. *Phys. Rev. B* **72**, 033414 (2005).
65. Wernsdorfer, W., Murugesu, M. & Christou, G. Resonant tunneling in truly axial symmetry Mn<sub>12</sub> single-molecule magnets: Sharp crossover between thermally assisted and pure quantum tunneling. *Phys. Rev. Lett.* **96**, 057208 (2006).

## Acknowledgements

This work is partially financed by ANR-PNANO, Contract MolSpintronics No. ANR-06-NANO-27 and by EC-RTN QUEMOLNA Contract No. MRTN-CT-2003-504880. L.B. acknowledges E.U. support through the EIF-041565-‘MoST’ Marie Curie fellowship.